

# An Irredundant and Compressed Data Layout to Optimize Bandwidth Utilization of FPGA Accelerators

Corentin Ferry  
Univ Rennes, CNRS, Inria, IRISA  
Rennes, France  
cferry@mail.colostate.edu

Nicolas Derumigny  
Colorado State University,  
Univ. Grenoble Alpes, Inria,  
CNRS, Grenoble INP, LIG  
38000 Grenoble, France  
nicolas.derumigny@inria.fr

Steven Derrien  
Univ Rennes, CNRS, Inria, IRISA  
Rennes, France  
Steven.Derrien@irisa.fr

Sanjay Rajopadhye  
Colorado State University  
Fort Collins, CO, USA  
First.Last@colostate.edu

## ABSTRACT

Memory bandwidth is known to be a performance bottleneck for FPGA accelerators, especially when they deal with large multi-dimensional data-sets. A large body of work focuses on reducing off-chip transfers, but few authors try to improve the efficiency of transfers. This paper addresses the latter issue by proposing (i) a compiler-based approach to accelerator’s data layout to maximize contiguous access to off-chip memory, and (ii) data packing and runtime compression techniques that take advantage of this layout to further improve memory performance. We show that our approach can decrease the I/O cycles up to  $7\times$  compared to un-optimized memory accesses.

## KEYWORDS

memory access, redundancy, data packing, padding, arbitrary precision, memory allocation

## 1 INTRODUCTION

FPGA accelerators have gained significant popularity in recent years, despite their inherent programming complexity. High-Level Synthesis tools play a pivotal role in reducing the design challenges associated with FPGA acceleration, and facilitate their adoption in new application domains (e.g. machine learning).

FPGA accelerator boards offer massive computational capabilities, but their performance is often hindered by an under-performing memory system, which becomes a performance bottleneck [16]. This is especially true for accelerators that target compute intensive kernels operating on large data-sets. This issue is generally addressed through program transformations that increase temporal reuse, trading off-chip memory transfers for on-chip storage resource. However, this approach does not primarily seek to optimize bandwidth usage (i.e. total amount of data transferred), leaving room for further improvement.

Another approach consists in improving the effectiveness of the memory subsystem by reorganizing access patterns and data layout in order to exploit FPGA-specific constraints[17]. One classical way of doing so is by exploiting large burst-based transfers, which requires contiguous data in memory. This is however not easy when dealing with the multi-dimensional data-sets found in

many applications, since the usual row-major and/or column major layouts only guarantee contiguity of data in only one dimension.

The problem becomes even more difficult when considering custom data formats (fixed/floating point) whose bitwidth do not correspond to the native memory bus interface. In such cases, the designer is left with two choices : padding the format to fit the bus width or deal with misaligned access, both choices incurring a loss of effective bandwidth.

Nevertheless, the ability to design application-specific hardware also brings opportunities to improve bandwidth efficiency. For example, the fact that successive and/or adjacent values are numerically close (typical case in physical simulation) makes runtime compression a viable strategy to increase the effectiveness of memory transfers.

In this paper, we present an automatic HLS optimisation flow that combines contiguity, data packing and compression to maximize the utilization of bandwidth with custom data types. More precisely, our contributions are the following:

- an algorithm to automatically derive (i) burst-friendly data layouts, and (ii) accelerator-specific access patterns that maximize contiguity while enabling data packing and compression,
- an automated code generation framework implementing the algorithm that generates synthesizable hardware,
- an evaluation of our approach on FPGA accelerators generated using the code generator that shows a up to  $7\times$  decrease in I/O cycles.

This paper is organized as follows: Section 2 presents the concepts and core optimization techniques our work is relying on; Section 3 describes the memory layout transformation, and Section 4 explains how we automatically apply it to FPGA accelerators. Finally, Section 5 validates our approach and discusses it on a series of benchmarks.

## 2 BACKGROUND

### 2.1 Locality optimizations

As manually optimizing an HLS design at the source level is a tedious process, automated approaches are now routinely used for HLS/FPGA targets in order to exploit parallelism and locality at

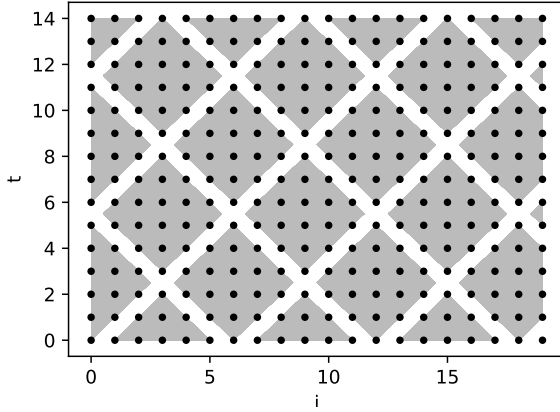


Figure 1: Domain of the Jacobi stencil divided into tiles of size  $6 \times 6$ . Each tile contains 18  $(t, i)$  points corresponding to 18 computations of  $c_{t,i}$ .

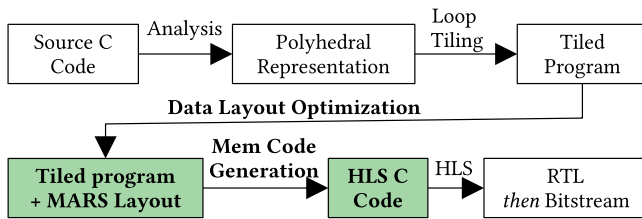


Figure 2: Compiler flow (our contributions in green)

multiple levels, which are often implemented as source-to-source compilers [5, 14, 15, 28]. Due to the inherent regularity of HLS-valid code, loop transformations engines such as PolyOpt/HLS [21] and POLSCA [29] excel at this task. However, such transformations are calibrated to improve computation time of benchmarks and do not seek to change the memory layout to enforce memory access contiguity.

Indeed, to get the best runtime performance from an FPGA accelerator, it is necessary to limit its off-chip memory accesses as much as possible. Only a fraction of large data sets can fit the limited size of on-chip memory; programs operating on large data sets must therefore be transformed to work on smaller workloads at a time. Loop tiling does this: it breaks large spaces into smaller sub-problems called *tiles*, where the on-chip memory and parallelism requirements of each tile match those available on the chip.

An accelerator for a tiled program processes the domain tile by tile. To execute a tile, the accelerator needs to retrieve intermediate results from previously executed tiles. These intermediate results are located outside of the accelerator, in off-chip memory, and need to be copied into on-chip memory.

The amount of on-chip memory needed to run a tile is directly influenced by the tile’s shape and size. In addition, when the tile size increases, the overall off-chip memory access is reduced, thus improving the overall arithmetic Intensity. Selection of the best tile

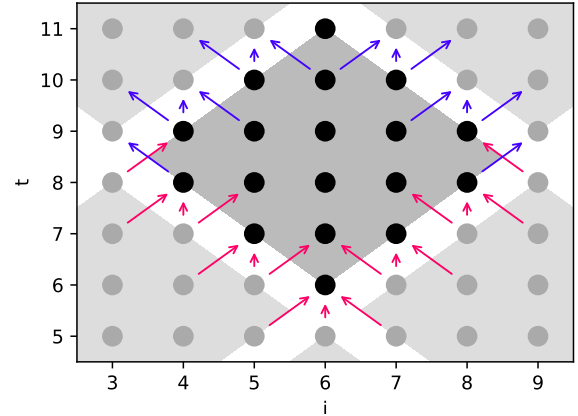


Figure 3: Inter-tile communication pattern for the Jacobi stencil: red arrows indicate data input into the tile shown in the center, and blue arrows indicate data output from this tile.

shape and size is outside the scope of this work, and mainly depends on the performance / area trade-off desired by the designer.

## 2.2 Illustrative example: 1D Jacobi stencil

To illustrate the flow proposed in this paper, we propose a Jacobi-1D stencil as running example. This kernel updates a one-dimensional sequence of values, and computes each point as a weighted average of it and its neighbors:

$$c_{t+1,i} = \frac{1}{3} (c_{t,i-1} + c_{t,i} + c_{t,i+1})$$

A C implementation of this stencil is provided in the PolyBench/C suite as the following code:

```

1 for (t = 0; t < _PB_TSTEPS; t++) {
2   for (i = 1; i < _PB_N - 1; i++)
3     B[i] = 0.33 * (A[i-1] + A[i] + A[i+1]);
4   for (i = 1; i < _PB_N - 1; i++)
5     A[i] = 0.33 * (B[i-1] + B[i] + B[i+1]);
6 }

```

This stencil operates over a two-dimensional iteration domain  $time \times space$  where each point has a coordinate  $(t, i)$ . Because such a domain may be arbitrarily large, the whole dataset may not fit into FPGA on-chip memory, and needs to be optimized before it can be mapped to the FPGA. As stated in the previous subsection, this naive implementation of Jacobi-1D cannot fit on-chip for gigabyte-scale problem sizes, thus requiring tiling. For the sake of simplicity of the illustration, we have chosen small, diamond-shaped tiles, illustrated in Figure 1.

For this tiling scheme, intermediate results to be retrieved come from the tiles located below the tile to execute; in Figure 3, these tiles are designated as the source of incoming arrows into the tile to execute. Likewise, the outgoing arrows show those intermediate results that will be used by other neighboring tiles. All of these data

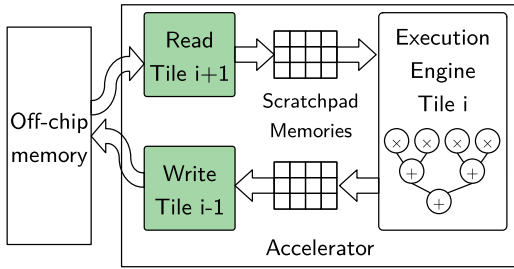


**Figure 4: Macro-pipeline structure: read-execute-write. Our contribution focuses on the read and write stages.**

transfers are the ones this work seeks to optimize; improvements of the compute engine fall out of the scope of this paper.

### 2.3 Deriving parallel accelerators using HLS

The optimizations mentioned section 2.1 are only a part of all those optimizations that need to be applied to get the best performance. One also needs to extract parallelism to maximize utilization of operators on the FPGA, and create a macro-pipeline to maximize the compute throughput.

Loop tiling naturally yields a “read-execute-writeback” macro-pipeline structure as illustrated in Figure 4: because tiles can be executed atomically, all I/O operations can happen before and after execution. HLS tools such as Vitis HLS support such macro-pipelines through manual code annotation, but through a restricted set of conditions of the pipeline (i.e. absence of cyclic dependency between stages). Moreover, automated macro-pipelining further increase pressure on the on-chip memory usage, as buffers used for inter-stage communication are either implemented using FIFOs or duplicated. While standard coding techniques would pass the complete tile data buffer across pipeline stages, this widely inefficient in hardware as communication only requires a subset of the actual tile data. On one tile of our Jacobi-1D example from subsection 2.2, the required data to be communicated is represented in blue in Figure 6.

Usually, the goal of the execute stage is to take advantage of massive operation-level parallelism (thanks to loop pipelining and unrolling), that have already been extensively addressed [4, 21, 22, 25]. In this paper, we only seek to optimize transfer times and memory bandwidth usage; optimisation of the complete design including crafting and balancing of a coarse-grain pipeline are not evaluated.

In applications with low operational intensity, the limited off-chip memory bandwidth turns the read and write stages into performance bottlenecks, even with aggressive tiling transformations. In most cases, this is due to a poor utilization of the off-chip memory interface, where only a fraction of the peak bandwidth is effectively used due to inefficient access patterns. As a matter of fact, approaching the peak memory bandwidth requires that almost all access to external memory consist of large transfers over contiguous memory locations (called memory *burst*).

HLS tools can infer burst memory accesses depending on the target interface. In the case of a shared bus (e.g. AXI, PCIe), which is commonly found for off-chip accesses, a *burst* access may occur

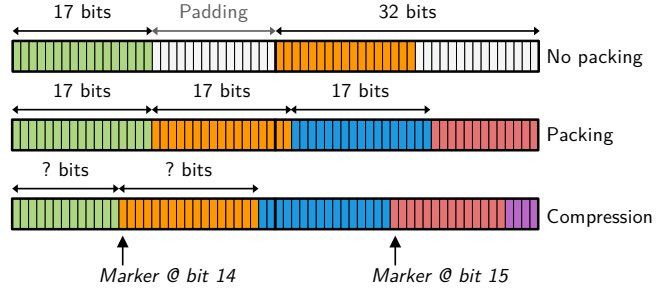


**Figure 5: Data packing and compression reduce storage and transfer redundancy at the expense of address alignment and, for compression, predictability of addresses.**

if the bus supports it and the compiler recognizes access to a series of consecutive addresses. Tools such as Vitis HLS 2022.2 exploit this using with either a call to a HLS-specific memcopy routine, or through some form or pattern matching in the source code. In burst mode, no cycle is spent stalling for a new value after a one-shot initialization latency, which yields full utilization of the available bandwidth.

The goal of this work is to propose a **source level compiler optimisation to (i) reorganize data in memory to enable contiguous burst access and (ii) further improve bandwidth utilization through packing and compression.** Our optimization pass is meant to be integrated within an HLS polyhedral compilation flow, as illustrated in Figure 2; aiming at sitting between the locality optimization phase (tiling) and the HLS synthesis stage. In fact, **our approach does not replace locality optimizations, it complements them.**

### 2.4 Padding vs packing

In order to maximize the utilization of bandwidth, every bit of data transmitted must be useful. However, with domain-specific data types (e.g., custom fixed point), unused bits must usually be transmitted due to memory alignment requirements. In the following, we explain how data contiguity can be leveraged to two ways: packing data to reduce the unused bits transmitted; and compressing data to further save bandwidth.

Most memories are byte-addressable and most processor architectures also require aligned accesses at word boundaries, usually at 32 or 64 bits. Although FPGA accelerators can operate on arbitrary-precision data types, off-chip data transfers must abide by the addressing requirements of the external memory. They therefore need to pad the incoming and outgoing data: in practice, for a 17-bit access, 32 bits of data will be transferred, 15 bits of them being wasted in padding.

Note that padding is necessary to enable random accesses to data: it provides the guarantee that a given memory cell contains only the requested data and no manipulation needs to be done to extract it. Data accessed in a contiguous manner does not need this guarantee and may overlap multiple adjacent cells, as simple wire manipulations on the FPGA will give back the original data.

Data packing, as illustrated in Figure 5, consists in avoiding padding the data so that words are adjacent at the bit level in memory. Figure 5 shows buffer structure for unpacked and packed data of 17 bits in 32-bit words. Unpacked data has aligned addresses, but requires extra storage and transfers unused data; packed data has unaligned addresses but saves storage and avoids some redundant bits from being transmitted. It becomes however impossible to randomly seek in a packed stream due to misalignment without additional data processing, but by definition such random seeks do not happen with contiguous accesses.

In our approach, we leverage contiguous accesses to (i) avoid the adverse effects of packing induced misalignment and (ii) to maximize bandwidth utilization by not padding data.

## 2.5 Runtime data compression

Packing data saves bandwidth by eliminating the padding bits, and is applied independently of the data itself. However, further optimisation is possible by exploiting properties of the data (e.g., correlation between integers in an array) for compression. When this technique is applied right before / after off-chip communications, the design benefits from a reduction of I/O cycles (as the amount of data transferred is reduced) without increase of the computation subsystem as the latency of the compression module can be hidden by the pipelining structure

Compression is easy to apply to contiguous streams of data, but is not to data where indexed or random accesses are necessary. We must exhibit access contiguity, as it is in general impossible to seek within a compressed block without decompressing more data than needed. Figure 5 shows that the position of data within a compressed block is unpredictable.

Our approach performs runtime compression and, to maximize its efficiency, creates data blocks with a contiguous access guarantee to ensure every decompressed piece of data is used.

In general, the compression algorithm is domain-specific, e.g., ADPCM for voice [6] or JPEG for images [24]. For FPGA implementations, the choice of the algorithm is also driven by its throughput: compression and decompression must be able to sustain the input and output throughput not to become the bottleneck. We choose to illustrate the idea with a simple differential compression algorithm which encodes a sequence  $w_0 w_1 \dots w_n$  of  $N$ -bit words as follows:

- Encode  $w_0$  as is.
- For  $1 \leq i \leq n$ :
  - (1) Compute  $\Delta = w_i - w_{i-1}$ ,
  - (2) Let  $L$  be the number of leading zeroes of  $\Delta$  if  $\Delta \geq 0$ , or leading ones if  $\Delta < 0$ ,
  - (3) Encode  $N - L$  using  $\lceil 1 + \log_2(N) \rceil$  bits, followed by the sign bit of  $\Delta$ ,
  - (4) Encode the  $N - (L + 1)$  lowest bits of  $\Delta$ .

This technique is especially effective when the distribution of the transferred data is not spread, typically on benchmarks based on the computation of the average such as our Jacobi-1D example from subsection 2.2.

## 3 MEMORY LAYOUT OPTIMIZATION

This work seeks to minimize the I/O cycles for an accelerator to transmit and retrieve its data into and from global memory. Locality

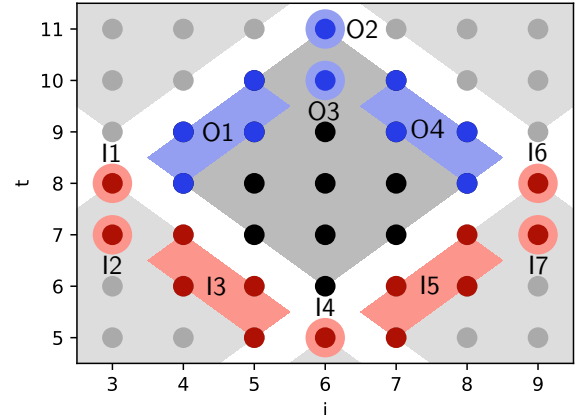


**Figure 6: MARS: Groups of points within a tile which data is contiguous in global memory. In blue, the MARS produced by the center tile (O1 to O4); in red, the MARS consumed by that same tile (I1 to I7).**

optimizations having already been applied, we do not want to store or retrieve *fewer* values from memory, but rather make *better* accesses to memory, from the bandwidth utilization, and therefore I/O cycles, standpoints.

To this aim, we build a **contiguous, irredundant and compressed data layout**. This section details the steps taken: first, we analyze the program and extract sets of on-chip data as contiguous data blocks; second, we lay out these data blocks to obtain further contiguous accesses; third, we compress and pack the data blocks together to save even more bandwidth.

### 3.1 Extracting Contiguous Data Blocks

The first step in our method consists in analyzing a program's behavior with respect to memory, to determine which data can/should be grouped together as contiguous blocks. The sought groups of data honor two properties:

- **Atomicity:** If any data in the group is needed for an instance of the accelerator's execution flow (a tile), then the entire group is also needed for the same tile.
- **Irredundancy:** No data is retrieved or stored more than once into memory throughout the execution of a single tile.

These groups of data are determined by using the analysis technique from Ferry et al. [9] within a polyhedral compiler. This analysis yields sets of on-chip memory addresses, such that all the data from these on-chip cells will be allocated a contiguous block of data in off-chip memory.

*Example.* Applying the MARS analysis from [9] to the Jacobi stencil of Section 2.2 gives the sets of addresses corresponding to the points illustrated in Figure 6:

- For the input of each tile, seven contiguous blocks of data labeled I1 to I7 are to be taken, across three different producer tiles.

- For the output, each tile will produce four contiguous blocks of data labeled O1 to O4.

There is a correspondence between output blocks (MARS)  $O_x$  from a tile and input blocks  $I_y$  from other tiles: each  $O_x$  corresponds to one  $I_y$  in several other tiles.

Without any further information, the result of MARS analysis would make the accelerator require seven input and four output burst accesses. This number could potentially be reduced. If I1, I2 and I3 were adjacent in memory, it would be possible to make a single access instead of three, and likewise for I5, I6 and I7. The total number of input accesses would go down to just three.

In order to reduce the number of accesses to the above, we have to show that it is actually achievable: the blocks I1 through I7 are read by multiple tiles, and coalescing opportunities for one tile may be incompatible with another tile’s coalescing opportunities.

The next subsection formalizes this example into an optimization problem seeking to minimize the number of accesses.

### 3.2 Enabling Coalesced Accesses across Contiguous Data Blocks

From the polyhedral analysis of the previous subsection, we have determined sets of on-chip data to be grouped as contiguous blocks of data, called MARS. How these blocks are laid out in memory is important for access performance: if multiple MARS happen to be accessed in a row and they are adjacent in memory, the accesses to these MARS can be coalesced into a single access and better utilize bandwidth.

This section explains how the “outer layout” of the MARS is determined so as to maximize the coalescing opportunities.

**3.2.1 Properties of the layout.** The goal of this work is to minimize the number of I/O cycles, and therefore the data layout must exhibit contiguity (for both reading and writing). However, that contiguity must not come at the price of an increase in I/O volume. To model this constraint, we apply two hypotheses.

**Contiguous tile-level allocation.** We are looking for a layout of MARS in memory, and know that compression will be applied to them. Due to the size and position of compressed blocks being unpredictable, it is not feasible to interleave MARS from multiple tiles in memory. Therefore, **we allocate each tile a contiguous block of memory for its MARS output.**

This allocation has two consequences: the write side can be done entirely contiguously, and we only have to optimize contiguity at the read side.

**Irredundancy of storage.** Under the previous hypothesis, we want to maximize the coalescing opportunities between MARS accesses for the read side only. While it is possible to obtain this contiguity by replicating the MARS in multiple layouts, one per consumer, doing so would defeat the goal to save I/O cycles. We therefore choose to **store each MARS only once in memory** (irredundant storage).

The goal is now to find a single layout for the MARS produced by each tile, that exhibits as much read-side coalescing opportunities as possible. We obtain it through an optimization problem that is defined in the next subsections.

**3.2.2 Example.** In the example of Section 3.1, it appeared that the number of burst accesses could go from 7 to 3. Let us show there actually exists a layout achieving these 3 bursts.

Figure 6 shows the correspondence between input and output MARS:

- I1, I2 and I3 come from the southwest tile, corresponding to its O2, O3 and O4 blocks. We would like these three MARS to be contiguous, regardless of which relative order, to make a single burst.
- I4 comes from the south tile, corresponding to its O2 block.
- I5, I6 and I7 come from the southeast tile, corresponding to its O1, O2 and O3 blocks. We would also like them to be contiguous.

We do not make any hypothesis on the relative location of data from the southwest tile, the south tile and the southeast tile. This makes it impossible to obtain fewer than 3 burst accesses.

The information we have at this point can be used as the constraints and objective of an optimization problem: we want to maximize the number of contiguities in the layout among those desired, under the irredundancy constraint. We provide a solver with the following problem:

- Maximize the contiguities among the desired ones: make MARS O2, O3 and O4 contiguous in any order, and make MARS O1, O2 and O3 also contiguous in any order.
- Per the hypothesis of Section 3.2.1, we want a layout of MARS O1, O2, O3 and O4.
- There can be no fewer read bursts than 3.

The solver returns the following layout of the output MARS for each tile: O1, O3, O2, O4.

Looking from the consumers, I1, I2 and I3 (resp. southwest O2, O3 and O4) are contiguous; I5, I6 and I7 (southeast O1, O2 and O3) are also contiguous. We can therefore coalesce, for each tile, the reads I1, I2 and I3 into a single burst, and I5, I6 and I7 into another burst, achieving the three sought input bursts.

**3.2.3 General case.** In this section, we lay out the blocks of data from the MARS analysis to maximize the coalescing opportunities between them.

With the allocation choice of Sec. 3.2.1, writes are guaranteed to be done without discontinuity. We therefore lay out the MARS to make the *read* side as contiguous as possible. In other words, we need to lay out the MARS in memory so that as many MARS as possible can be read as a *coalesced* burst.

We propose to model this problem as an Integer Linear Programming optimization problem as described in Algorithm 1. Intuitively, if a pair of MARS is needed by a consumer tile and the two MARS are next to each other in memory, then a coalesced access for the two (a “contiguity”) is issued. We therefore seek to maximize the number of such contiguities.

The solution to this optimization problem, given by the solver is an ordered list of the MARS produced by each tile, that allows the minimal number of transactions to read all MARS input of a tile.

The layout created in this section honors the *irredundancy* property of the MARS (see Section 3.1), but does not yet take full advantage of their *atomicity*: the fact that the MARS are contiguous



**Algorithm 1:** Optimizing the MARS layout

---

**Input:**  $M_I = (m_i) : i = 1, \dots, N$  = list of MARS,  
 $\mathcal{P}$  = list of producer tiles from which MARS are needed,  
**Result:**  $M_O$  = ordered list of MARS  
**Optimization Variables:**  
**let**  $\delta_{i,j} \in \{0, 1\}$  = successor variables:  $\delta_{i,j} = 1$  encodes that MARS  $i$  is immediately before MARS  $j$  in memory.  
**let**  $\gamma_i \in \{1, \dots, N\}$  be a permutation;  $\gamma_i$  is the position where MARS  $i$  will be in the final layout.  
**Problem Constants:**  
**let**  $a_{p,i,j}$  be equal to 1 if  $m_i$  and  $m_j$  ( $i, j \in [[1, N]]$ ) from tile  $p \in \mathcal{P}$  are consumed together, 0 otherwise.  
**Maximize** #{contiguities}:  $\sum_{p \in \mathcal{P}} \sum_{i=1}^N \sum_{j=1, j \neq i}^N a_{p,i,j} \delta_{i,j}$  **subject to:**

- $\forall i : \delta_{i,i} = 0$  (a MARS is not its own predecessor)
- $\forall i : \sum_j \delta_{i,j} \leq 1$  (a MARS has at most 1 predecessor)
- $\forall j : \sum_i \delta_{i,j} \leq 1$  (a MARS has at most 1 successor)
- $\sum_i \sum_j \delta_{i,j} = N - 1$  (number of successor relations)
- $\forall i : 0 \leq \gamma_i \leq N - 1$  (permutation of length  $N$ )
- $\forall i, j : (\gamma_j - \gamma_i = 1) \Leftrightarrow (\delta_{i,j} = 1)$  (definition of successor)
- $\forall i, j : (i \neq j) \Rightarrow |\gamma_i - \gamma_j| \geq 1$  (MARS have  $\neq$  positions)

**return**  $M_O = (m_{\gamma(1)}, \dots, m_{\gamma(N)})$  ( $\gamma$ -ordered list of MARS)

---

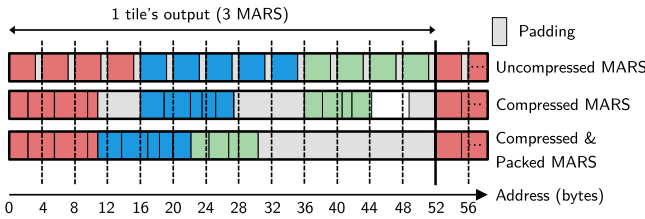


**Figure 7:** MARS data shown without compression, with compression (inside the MARS) and with MARS compression and packing. Packing the compressed MARS preserves the contiguity of coalesced accesses.

blocks of data makes them ideal candidates for data packing and compression. This is what we perform in the next subsection.

### 3.3 Contiguity-Preserving Block Compression

So far, our approach has given a layout of data in memory enabling coalesced accesses to contiguous blocks of data produced and consumed by an accelerator. These blocks have an atomicity property that we can further exploit to save bandwidth, by applying data packing and compression, as illustrated in Figure 7.

**3.3.1 Combining compression and packing.** Compressed blocks of data must be considered atomic in the sense that no random accesses into them are possible. This atomicity property is borne by the MARS, as each MARS data block is entirely used when it is accessed, i.e. there are no partial accesses to a MARS.

Compressing the MARS reduces the size of the data and therefore saves bandwidth and storage space; however, it can also break the contiguity brought by the layout of Section 3.2 as illustrated by Figure 7. To preserve it, we also apply *packing* to the compressed MARS, making them immediately adjacent to each other in memory.

Packing compressed MARS also spares the accelerators from unused reads due to padding.

**3.3.2 Need to preserve metadata.** As the size of compressed blocks depends on their data, it is impossible to know the exact size of each access. However, the size of a burst access must be known prior to the request being issued; additionally, using an estimation of the size or an over-approximation would result in unused input data or additional requests to fill in missing data.

In order to be able to exactly fetch the right size, it is necessary to keep track of the size of each compressed MARS. Moreover, the packing of compressed MARS means that the start of a compressed block may be improperly aligned. It is also therefore necessary to keep track of the alignment of each MARS for proper decompression. In our implementation, bookkeeping is done using on-chip *markers* that are filled in after each MARS is compressed. Details are in Section 4.2.2.

Packing will cause unused input data to enter; however, its size is bounded to one aligned word at the beginning and one aligned word at the end of each transaction. This input redundancy is notably independent of the size of the MARS.

## 4 INTEGRATION INTO HLS DESIGN FLOW

In this section, we show how we transform an HLS accelerator description in order to optimize its off-chip memory accesses for bandwidth utilization.

The off-chip data layout and compression proposed in Section 3 can be automatically implemented around the existing description of a tile in HLS. The result is a sequence of steps:

- Read MARS layout data and non-MARS input data from off-chip memory into on-chip FIFOs,
- Decompress the input data into FIFOs,
- Dispatch MARS data into on-chip buffers with an allocation suitable for computation,
- Perform the computations onto on-chip buffers,
- Collect MARS output data from the on-chip buffers into FIFOs,
- Compress the collected data,
- Write back the results into MARS layout in off-chip memory.

The next subsections explain how the complex data structures describing the MARS are turned into two simple decompression/dispatch and collect/compression steps.

### 4.1 From MARS to Collect/Dispatch Functions

The input and output data of each tile is respectively copied into and out of on-chip buffers before the tile execution takes place and after it has fully completed. This is the step where the data goes from a contiguous layout to a non-contiguous layout (suitable for execution) and vice-versa.

Implementing these dispatch and collect steps requires to describe each MARS so that the data contained in it is placed into, or taken from, the right location in on-chip memory. Before dispatch and after collect, the data is located into FIFOs in the contiguous layout.

```

1 // MARS Dispatch
2 for(int i=0; i<33; ++i) {
3   // take on-chip address from ROM
4   struct mars_transfert mt = FPGA_MARS_IN_TBL[i];
5   switch (mt.array) {
6     // on-chip random write
7     case MARS_DATA_ENUM::A: {
8       marsToMem_A(mt.dim0, mt.dim1);
9       break;
10    }
11    case MARS_DATA_ENUM::B: {
12      marsToMem_B(mt.dim0, mt.dim1);
13      break;
14    }
15  }
16 }

```

**Figure 8: Structure of the MARS dispatch implementation (off-chip to on-chip layout)**

MARS can have arbitrary complex shapes, and cannot in general be described using simple loops. However, it is possible to fully unroll these loops and obtain a list of on-chip addresses for each MARS. Such unrolled lists are placed into read-only memories on chip. Iterating through these ROMs as in Figure 8 gives the corresponding addresses. The size of these ROMs is notably only dependent on the tile size, and not on the problem size or data type.

## 4.2 Automatic compression

When the data is in the contiguous layout in the form of MARS, it can be seamlessly compressed and decompressed, and the compressed MARS can be packed to preserve contiguity. We explain here the compression, packing and decompression steps, along with how the compression metadata is taken care of.

**4.2.1 Compressing Data and Packing MARS.** The compression step is relatively straightforward: the compression module takes its input from the collect step FIFO, and generates a compressed stream of data from it. The layout of the data in this FIFO is not altered by the compression step. Likewise, the decompression step takes a stream of compressed words and decompresses it into a FIFO, which is then used by the MARS dispatch step. MARS packing is transparently implemented by the compression step: because MARS are provided in a contiguous manner from the collect step, the first word of each MARS will be immediately adjacent to the last word of the previous MARS in the compressed data stream.

Our compressor, which algorithm is given in Section 2.5, is pipelined with an initiation interval of 1 cycle, despite a loop-carried dependence.

The difficult part to implement is decompression: because not all MARS from a given tile are decompressed, we need to be able to seek at the start of a particular MARS. This ability is given by metadata described in the next paragraph.

**4.2.2 Metadata management.** The consequence of MARS compression is that their size is unknown a priori. To preserve the contiguity of the layout from Section 3.2, we must avoid padding the compressed MARS to preserve alignment. Therefore, the compressed

MARS are packed and immediately adjacent to each other in memory.

To keep track of the position of each MARS, we use a data structure with two pieces of information: a *coarse-grain* position indicating how far (in aligned words) to seek, and a *fine-grain* position marker that specifies which bit is the first of the said MARS.

Because the length of MARS is known at compile time and constant across tiles, the position of the markers within the uncompressed stream is also constant. Therefore, like the MARS descriptions, the positions of markers (i.e. start of each MARS) within the uncompressed stream are put into a ROM:

```

1 #define NB_MARKERS 3
2 #define MARKERS {62, 63, 64}

```

The markers for the compressed stream are maintained within an on-chip cache, which size is specified at synthesis time via a macro:

```

1 struct compressed_marker<NB_MARS_POS_BITS,
2   LOG_BUS_WIDTH> markers[COMPRESSION_METADATA_SIZE][
3   NB_MARKERS];

```

The allocation within this cache is done from the host: registers are used to specify whether a tile’s MARS are compressed, whether its dependences are, and where the markers for its dependences are located. This location depends on the size of the space; for the Jacobi stencil, the formula is:

```

1 unsigned compressionMetadataAllocation(
2   int tsteps, int n, int M1, int M2, int k1, int k2) {
3   return (k2) + M2DEC_FORMULA + M2 * ((k1 - 1) & 0x01);
4 }

```

It should be noted that the markers structure is persistent between runs. It is updated by the MARS write step and used by the MARS read step. This update prevents the current HLS tools from constructing a macro-pipeline (e.g. using the HLS DATAFLOW pragma) unless the structure is in a separate module.

## 4.3 Host/FPGA dispatching of tiles

The FPGA accelerator must have a simple control structure to exhibit as much parallelism as possible. Therefore, only *full tiles* are executed on FPGA. Full tiles also all have the same volume of I/O, regardless of their position in the iteration space.

Partial tiles, i.e. those that contain space boundaries, are run on the host CPU, using the original program’s allocation. To permit this, data computed on FPGA is taken back from MARS into the original program’s memory, and MARS are created back from partial tiles results. It can be demonstrated that no FPGA tiles need any missing MARS data from partial tiles, and therefore there is no issue in writing part of the MARS for these tiles.

The operations performed to execute a partial tile (on the host) are:

- Read MARS from neighboring full tiles that were executed on FPGA, remap their data to its original location,
- Execute the tile’s iterations using the original allocation,
- Write back MARS by copying data from the original allocation, skipping cells that would be in MARS yet have no producer iteration.

The control flow necessary for compression would significantly lengthen the execution of host tiles. Therefore, only tiles which producers and consumers are all executed on FPGA will use compression.

## 5 EVALUATION

We evaluate our approach with respect to the following questions:

- **Compile-time performance:** How much time does it take to compute the MARS layout?
- **Design quality:** How does using MARS affect the FPGA accelerator’s area consumption?
- **Runtime performance:** How much I/O cycles do compressed MARS save with respect to a non-MARS memory layout?
- **Applicability:** How does the data type, tile size and problem size affect the compression ratio?

### 5.1 Protocol and benchmarks

*5.1.1 Benchmarks.* We have selected the following applications from the PolyBench/C suite[20]:

- *jacobi-1d:* Jacobi 1D stencil, as used in the running example;
- *jacobi-2d:* Two-dimensional version of the Jacobi stencil, exhibiting few and simple MARS;
- *seidel-2d:* More complex benchmark exhibiting a higher number of MARS with more complex shapes.

Layout determination was done using the Gurobi solver (version 10.0.3 build v10.0.3rc0 (linux64)).

The data types used are fixed-point numbers (18 bits, 24 bits, 28 bits) and floating-point numbers (float, double). We also ran simulations with a 12-bit fixed-point data type without synthesizing it, Vitis HLS being unable to infer bursts from that data type.

The chosen applications provide a non-MARS data layout in their original code. Because FPGA developers usually try to seek burst accesses where possible, we have created two access patterns on the non-MARS layout to compare against that try to exhibit bursts:

- A minimal access pattern, fetching and storing the exact I/O footprint of the tile, letting the HLS tool infer bursts where possible.
- A rectangular bounding box of the accessed data like done in PolyOpt/HLS [21], which description is simple enough to infer only burst accesses.

Both access patterns are generated using a polyhedral code generator available in ISL [27].

*5.1.2 Hardware platform.* We used a Xilinx ZCU104 evaluation board, equipped with a xczu7ev MPSoC. We ran Pynq 3.0.1 with Linux 5.15 and synthesis was done using the Vitis/Vivado suite version 2022.2.2 All benchmarks, are running at a clock frequency of 187 MHz and communicate with the off-chip DDR using one non cache-coherent AXI HP port.

*5.1.3 Protocol.* Each benchmark is run for each data type, each space size and tile size. Part of the computation is done on the host: incomplete tiles are executed on a single thread on the Cortex-A53

CPU of the MPSoC. Transfer cycles are measured only for the FPGA tiles and do not account for the host.

Cycle measurements are gathered using an on-FPGA counter and the area measurements are extracted from Vivado place and route reports.

Table 1 shows the characteristics of each benchmark, in terms of number of MARS, and number of bursts after coalescing optimization of Sec. 3.2.

### 5.2 Results and discussion

*5.2.1 Compile-time performance.* Table 2 shows the time it took for each benchmark to be run through the layout determination and code generation framework. The compilation process does not take more than a few seconds to execute for the benchmarks we selected, starting from the polyhedral representation of the program to the end of HLS code generation. Notably, the layout determination ILP problem only depends on the number of MARS and is independent of the tile size.

*5.2.2 Design quality.* Figure 9 shows the total area occupied by our benchmarks, with respect to the different memory allocation baselines. One tile size per benchmark is considered.

MARS introduces extra control logic and extra I/O functions that the other baselines do not have. It is therefore normal to observe area increases with this baseline. The most significant increases in Figure 9a are for *jacobi 1d*; in this benchmark, on-chip arrays are implemented in logic instead of Block RAM. Figure 9b shows little DSP and BRAM consumption by this benchmark compared to others. FIFOs holding all the MARS are implemented only on the MARS baseline, and require extra BRAMs. The extra DSP blocks for MARS baselines come from the address computations that are performed inside the I/O units; the size of the space is passed as a parameter instead of being a constant, requiring true multipliers.

Figure 9a shows that the data width causes the logic area to increase with it. This increase is more sensible in *jacobi 1d* where the on-chip arrays are implemented in logic instead of Block RAM, which effect is also visible in Figure 9b.

*5.2.3 Runtime performance.* Figure 10 shows the transfer time relative to compressed MARS for each data type and each benchmark.

*Impact of dimensionality.* For the 2d examples that have three-dimensional iteration spaces, using MARS layout is already profitable versus the non-MARS layouts; most of the gains are due to contiguity more than compression. On the one-dimensional Jacobi example, the gains are on the contrary more due to compression: the data being one-dimensional, non-MARS layouts are already contiguous. For small tile sizes like  $6 \times 6$ , the gains are marginal if any: the number of compressed elements is too small to exhibit large gains from compression.

*Effect of data type.* On the *jacobi-1d* benchmark, the choice of a  $200 \times 200$  tile size shows a more significant benefit in using compressed MARS for fixed-point data types than floating-point. This is explained with the better compression ratio: when modeling continuous spaces like those used on the Jacobi stencils, neighboring fixed-point values will have more higher bits in common than



| Benchmark | Tile Sizes                                       | #MARS In | #MARS Out | Read bursts | Write bursts |
|-----------|--|----------|-----------|-------------|--------------|
| jacobi-1d | $6 \times 6$ $64 \times 64$ , $200 \times 200$   | 7        | 4         | 3           | 1            |
| jacobi-2d | $4 \times 5 \times 7$ , $10 \times 10 \times 10$ | 28       | 13        | 10          | 1            |
| seidel-2d | $4 \times 10 \times 10$                          | 33       | 13        | 10          | 1            |

**Table 1: Characteristics of the selected benchmarks. The number of bursts per tile accounts for layout-induced access coalescing and is independent of tile and problem size.**

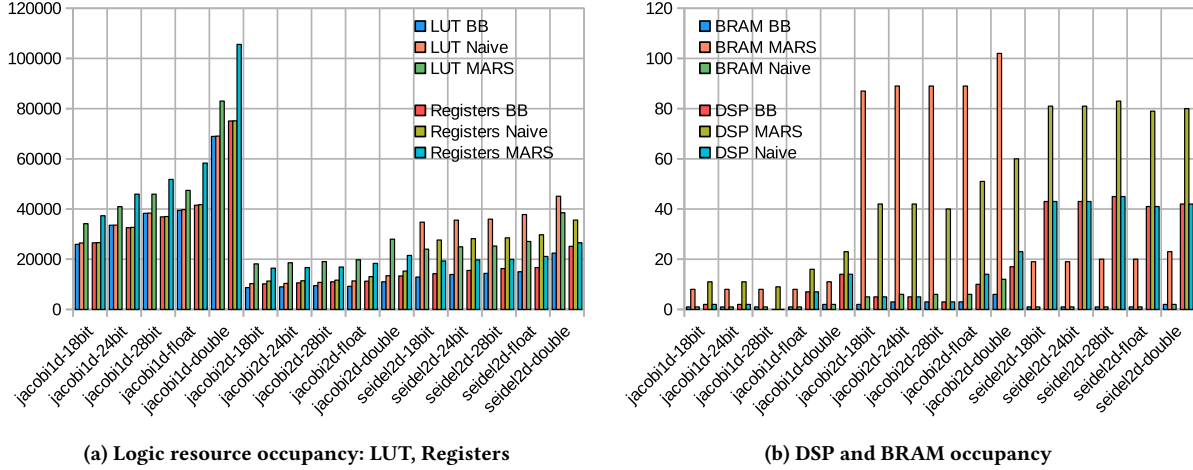


**Figure 9: Area statistics for the benchmarks**

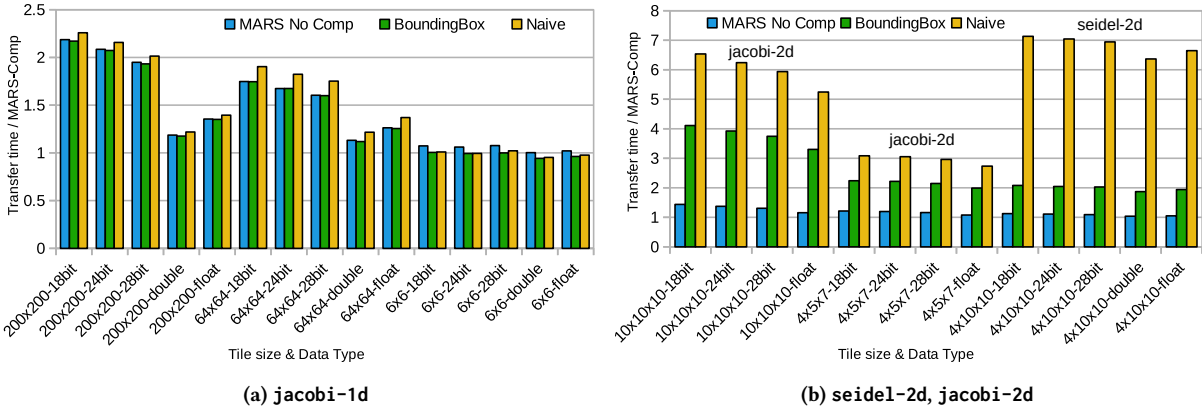


**Figure 10: Transfer time relative to compressed MARS (lower is better).**

| Benchmark | Tile Size                | Compile Time (s) |
|-----------|--------------------------|------------------|
| jacobi-1d | $6 \times 6$             | 0.76             |
| jacobi-1d | $64 \times 64$           | 0.68             |
| jacobi-1d | $200 \times 200$         | 1.02             |
| jacobi-2d | $4 \times 5 \times 7$    | 5.57             |
| jacobi-2d | $10 \times 10 \times 10$ | 5.09             |
| seidel-2d | $4 \times 10 \times 10$  | 3.21             |

**Table 2: Layout Computation and Code Generation Time**

floating-point data where neighboring values mostly only share the exponent.

**5.2.4 Applicability.** Figure 11 shows the compression rate for each data type and tile size for the jacobi1d benchmark. Two ratios are shown: the *true ratio* which accounts only for the bit savings due to compression, and a *ratio with padding* that accounts for the savings due to not padding the data. The ratio with padding is the one our accelerators really benefit from, because the data is not packed in memory except in compressed MARS form.

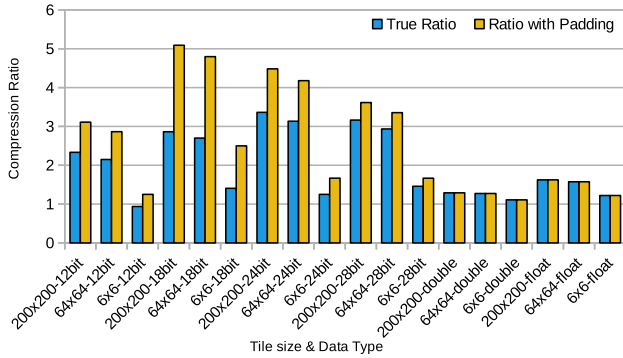


**Figure 11: Compression ratio vs. data type and tile size for jacobi1d**

Overall, compressing the data for the selected benchmarks is almost always profitable, possibly largely as the compression ratio goes up to 5.09:1 for  $200 \times 200$  tiles and 18-bit type.

We can observe that large tiles ( $64 \times 64$ ,  $200 \times 200$ ) exhibit closer compression ratios than smaller tiles ( $6 \times 6$ ). This discrepancy can be explained by the compressed chunks being too small to benefit from the data’s low entropy; for the smallest data type and tile size, compressing data is even worse than not compressing.

## 6 RELATED WORK

This work comes as part of a global effort to relieve memory-boundness of high-performance accelerators. In this section, we study other techniques used to relieve the memory wall, some of which may not apply to compilers due to not being automatable or breaking program semantics.

### 6.1 Data Compression

Data compression saves bandwidth without requiring to modify the program’s algorithm. It is therefore suitable for many bandwidth-bound problems.

*6.1.1 Compression techniques.* Data compression in FPGA accelerators is already a necessity for some intrinsically memory-bound applications such as deep convolutional networks, as no locality optimization can bring further bandwidth savings. We here focus on two kinds of compression: lossless and lossy.

*Lossless compression.* Lossless compression guarantees that the decompressed data is exactly the same as the data before it was compressed. This property makes it possible to do seamless, in-line compression and decompression as is done for MARS. This is commonly performed in deep neural network accelerators [1, 11]

Sparse encoding can be considered a form of lossless compression, and is also commonly found in machine learning applications [8, 13]. Sparse data structures often require indirections, which make them unsuitable for use in polyhedral compiler flows unless the sparse structure is immutable [12].

*Lossy compression.* It is possible to save more storage and bandwidth by using lossy compression. Some applications in machine

learning can afford a loss of precision without degrading the quality of the result, e.g. using JPEG-compressed images [18] as inputs. However, automatic compression alters the data and cannot be automatically inserted by a compiler unless the user explicitly requests it.

*6.1.2 Dynamic data compression.* In this work, we automate the compression and decompression of data and it is transparent to the computation engine on FPGA. Other works [19, 23] perform dynamic, demand-driven compression without prior knowledge of the data to be handled. Thanks to the static control flow of polyhedral codes, all the data flow is statically known and it is not necessary to maintain a cache policy.

## 6.2 Memory access optimization

The layout we propose in this work optimizes memory accesses by exhibiting contiguity using polyhedral analysis. In this section, we go through other polyhedral memory access optimizations, and explain other non-polyhedral ways it is possible to improve memory accesses.

*6.2.1 Polyhedral-based optimizations.* Using the polyhedral model and loop tiling to capture the data flow is the subject of a number of works, proposing different breakups of the dataflow. Datharthri et al. [7] and Bondhugula [2] propose decompositions of the inter-tile communications to minimize MPI communications. This work also seeks to optimize the passing of intermediate results, but the data allocation is not statically determined like in this work.

A MARS-like decomposition of the inter-tile data flow into coarse-grain blocks for MPI has been proposed by Zhao et al. [30]; our work achieves irredundancy which requires a finer-grain modeling than the one proposed by [30].

*6.2.2 Domain-specific optimizations.* Memory access optimizations such as a change of data layout or access pattern can also be specific to each problem. We show here two cases of domain-specific optimizations.

*Data blocking.* Data blocking (or tiling) is memory layout transformation that chunks multi-dimensional arrays into contiguous blocks. Similar to loop tiling, data blocking allows to coalesce accesses to entire regions of the input or output data.

Data blocking can be efficient when the memory footprint of one iteration of an accelerator corresponds to a data tile. Although it has been used to optimize machine learning accelerators [26], it may break spatial locality and degrade performance of accesses that cross tile boundaries.

Data blocking can be combined with loop tiling and polyhedral analysis to coalesce inter-tile accesses. Ferry et al. [10] seeks to exhibit the largest possible contiguous units spanning multiple tiles.

*Stencil optimization.* Stencil computations have regular and statically known memory access patterns. Domain-specific optimizers like SODA [3] derive an optimized FPGA architecture and memory layout specific to each stencil.

## 7 CONCLUSION

This work gives a twofold contribution: a compression-friendly, contiguous data layout, and an automated adaptation of FPGA accelerators to use this layout thanks to polyhedral compilation tools. Thanks to the compression and contiguity, we can automatically reduce the number of I/O cycles spent by the accelerator.

## REFERENCES

- [1] Thea Aarrestad, Vladimir Loncar, Nicolò Ghielmetti, Maurizio Pierini, Sioni Summers, Jennifer Ngadiuba, Christoffer Petersson, Hampus Linander, Yutaro Iiyama, Giuseppe Di Guglielmo, Javier Duarte, Philip Harris, Dylan Rankin, Sergo Jindariani, Kevin Pedro, Nhan Tran, Mia Liu, Edward Kreinar, Zhenbin Wu, and Duc Hoang. 2021. Fast convolutional neural networks on FPGAs with hls4ml. *Machine Learning: Science and Technology* 2, 4 (jul 2021), 045015. <https://doi.org/10.1088/2632-2153/ac0ea1>
- [2] Uday Bondhugula. 2013. Compiling Affine Loop Nests for Distributed-Memory Parallel Architectures. In *Proceedings of the International Conference on High Performance Computing, Networking, Storage and Analysis*. ACM. <https://doi.org/10.1145/2503210.2503289>
- [3] Yuze Chi, Jason Cong, Peng Wei, and Peipei Zhou. 2018. SODA: Stencil with optimized dataflow architecture. In *2018 IEEE/ACM International Conference on Computer-Aided Design (ICCAD)*. IEEE, 1–8. <https://doi.org/10.1145/3240765.3240850>
- [4] Young-kyu Choi and Jason Cong. 2018. HLS-based optimization and design space exploration for applications with variable loop bounds. In *2018 IEEE/ACM International Conference on Computer-Aided Design (ICCAD)*. IEEE, 1–8.
- [5] Jason Cong, Muhuan Huang, Peichen Pan, Yuxin Wang, and Peng Zhang. 2016. Source-to-source optimization for HLS. *FPGAs for Software Programmers* (2016), 137–163.
- [6] P Cummiskey, Nikil S. Jayant, and James L. Flanagan. 1973. Adaptive Quantization in Differential PCM Coding of Speech. *Bell System Technical Journal* 52 (09 1973). <https://doi.org/10.1002/j.1538-7305.1973.tb02007.x>
- [7] Roshan Dathathri, Chandan Reddy, Thejas Ramashekar, and Uday Bondhugula. 2013. Generating Efficient Data Movement Code for Heterogeneous Architectures with Distributed-Memory. In *Proceedings of the 22nd International Conference on Parallel Architectures and Compilation Techniques*. IEEE. <https://doi.org/10.1109/PACT.2013.6618833>
- [8] Yixiao Du, Yuwei Hu, Zhongchun Zhou, and Zhiru Zhang. 2022. High-Performance Sparse Linear Algebra on HBM-Equipped FPGAs Using HLS. In *Proceedings of the 2022 ACM/SIGDA International Symposium on Field-Programmable Gate Arrays*. ACM. <https://doi.org/10.1145/3490422.3502368>
- [9] Coentrin Ferry, Steven Derrien, and Sanjay Rajopadhye. 2023. Maximal Atomic Irredundant Sets: a Usage-based Dataflow Partitioning Algorithm. In *13th International Workshop on Polyhedral Compilation Techniques (IMPACT'23)*.
- [10] Coentrin Ferry, Tomofumi Yuki, Steven Derrien, and Sanjay Rajopadhye. 2022. Increasing FPGA Accelerators Memory Bandwidth with a Burst-Friendly Memory Layout. *IEEE Transactions on Computer-Aided Design of Integrated Circuits and Systems* (2022), 1–1. <https://doi.org/10.1109/tcad.2022.3201494>
- [11] Yijin Guan, Ningyi Xu, Chen Zhang, Zhihang Yuan, and Jason Cong. 2017. Using Data Compression for Optimizing FPGA-Based Convolutional Neural Network Accelerators. In *Lecture Notes in Computer Science*. Springer International Publishing, 14–26. [https://doi.org/10.1007/978-3-319-67952-5\\_2](https://doi.org/10.1007/978-3-319-67952-5_2)
- [12] Marcos Horro, Louis-Noël Pouchet, Gabriel Rodríguez, and Juan Touriño. 2023. Custom High-Performance Vector Code Generation for Data-Specific Sparse Computations. In *Proceedings of the International Conference on Parallel Architectures and Compilation Techniques (Chicago, Illinois) (PACT '22)*. Association for Computing Machinery, New York, NY, USA, 160–171. <https://doi.org/10.1145/3559009.3569668>
- [13] Shiqing Li, Di Liu, and Weichen Liu. 2023. Efficient FPGA-based Sparse Matrix-Vector Multiplication with Data Reuse-aware Compression. *IEEE Transactions on Computer-Aided Design of Integrated Circuits and Systems* (2023), 1–1. <https://doi.org/10.1109/tcad.2023.3281715>
- [14] Junyi Liu, Samuel Bayliss, and George A Constantinides. 2015. Offline synthesis of online dependence testing: Parametric loop pipelining for HLS. In *2015 IEEE 23rd Annual International Symposium on Field-Programmable Custom Computing Machines*. IEEE, 159–162.
- [15] Junyi Liu, John Wickerson, Samuel Bayliss, and George A Constantinides. 2017. Polyhedral-based dynamic loop pipelining for high-level synthesis. *IEEE Transactions on Computer-Aided Design of Integrated Circuits and Systems* 37, 9 (2017), 1802–1815.
- [16] Michael Lo, Young-kyu Choi, Weikang Qiao, Mau-Chung Frank Chang, and Jason Cong. 2023. HMLib: Efficient Data Transfer for HLS Using Host Memory. In *Proceedings of the 2023 ACM/SIGDA International Symposium on Field Programmable Gate Arrays*. 50–50.
- [17] Florian Mayer, Julian Brandner, and Michael Philippsen. 2023. Employing Polyhedral Methods to Reduce Data Movement in FPGA Stencil Codes. In *International Workshop on Languages and Compilers for Parallel Computing*. Springer, 47–63.
- [18] Hiroki Nakahara, Zhiqiang Que, and Wayne Luk. 2020. High-Throughput Convolutional Neural Network on an FPGA by Customized JPEG Compression. In *2020 IEEE 28th Annual International Symposium on Field-Programmable Custom Computing Machines (FCCM)*. 1–9. <https://doi.org/10.1109/FCCM48280.2020.00010>
- [19] O. Ozturk, M. Kandemir, and M.J. Irwin. 2009. Using Data Compression for Increasing Memory System Utilization. *IEEE Transactions on Computer-Aided Design of Integrated Circuits and Systems* 28, 6 (jun 2009), 901–914. <https://doi.org/10.1109/tcad.2009.2017430>
- [20] Louis-Noël Pouchet and Tomofumi Yuki. 2016. PolyBench/C 4.2.1. <http://polybench.sf.net>
- [21] Louis-Noël Pouchet, Peng Zhang, P. Sadayappan, and Jason Cong. 2013. Polyhedral-based data reuse optimization for configurable computing. In *Proceedings of the ACM/SIGDA international symposium on Field programmable gate arrays - FPGA '13*. ACM Press. <https://doi.org/10.1145/2435264.2435273>
- [22] Tiago Santos and João MP Cardoso. 2020. Automatic selection and insertion of hls directives via a source-to-source compiler. In *2020 International Conference on Field-Programmable Technology (ICFPT)*. IEEE, 227–232.
- [23] Somayeh Sardashti, Andre Sez nec, and David A. Wood. 2016. Yet Another Compressed Cache: A Low-Cost Yet Effective Compressed Cache. *ACM Trans. Archit. Code Optim.* 13, 3, Article 27 (Sept. 2016), 25 pages. <https://doi.org/10.1145/2976740>
- [24] A. Skodras, C. Christopoulos, and T. Ebrahimi. 2001. The JPEG 2000 still image compression standard. *IEEE Signal Processing Magazine* 18, 5 (2001), 36–58. <https://doi.org/10.1109/79.952804>
- [25] Atefeh Sohrabzadeh, Cody Hao Yu, Min Gao, and Jason Cong. 2022. AutoDSE: Enabling software programmers to design efficient FPGA accelerators. *ACM Transactions on Design Automation of Electronic Systems (TODAES)* 27, 4 (2022), 1–27.
- [26] Teng Tian, Xi Jin, Letian Zhao, Xiaotian Wang, Jie Wang, and Wei Wu. 2020. Exploration of Memory Access Optimization for FPGA-based 3D CNN Accelerator. In *2020 Design, Automation & Test in Europe Conference & Exhibition (DATE)*. 1650–1655. <https://doi.org/10.23919/DATE48585.2020.9116376>
- [27] Sven Verdoolaege. 2010. isl: An Integer Set Library for the Polyhedral Model. In *Mathematical Software – ICMS 2010*, Komei Fukuda, Joris van der Hoeven, Michael Joswig, and Nobuki Takayama (Eds.). Springer Berlin Heidelberg, Berlin, Heidelberg, 299–302.
- [28] Hanchen Ye, Cong Hao, Jianyi Cheng, Hyunmin Jeong, Jack Huang, Stephen Neuendorffer, and Deming Chen. 2022. Scalehls: A new scalable high-level synthesis framework on multi-level intermediate representation. In *2022 IEEE International Symposium on High-Performance Computer Architecture (HPCA)*. IEEE, 741–755.
- [29] Ruizhe Zhao, Jianyi Cheng, Wayne Luk, and George A Constantinides. 2022. POLSCA: Polyhedral High-Level Synthesis with Compiler Transformations. In *2022 32nd International Conference on Field-Programmable Logic and Applications (FPL)*. IEEE, 235–242.
- [30] Tuowen Zhao, Mary Hall, Hans Johansen, and Samuel Williams. 2021. Improving communication by optimizing on-node data movement with data layout. In *Proceedings of the 26th ACM SIGPLAN Symposium on Principles and Practice of Parallel Programming*. ACM. <https://doi.org/10.1145/3437801.3441598>